Received: 23 May 2025 | Revised: 23 September 2025 | Accepted: 6 October 2025

DOI: 10.1111/bph.70247

RESEARCH ARTICLE

Transcriptional and functional effects of mavacamten in multiple porcine and human models with hypertrophic cardiomyopathy

Elisa Kiselev[1] | Wilson Agyapong[1] | Bjarne Jürgens[1] | Elisa Mohr[1] | Shambhabi Chatterjee[1] | Hannah J. Hunkler[1] | Jawad Salman[2] | Giuseppe Cipriano[1] | Marco Bentele[1] | Junqing Liu[1] | Jonas Specht[1] | Kaja S. Menge[1] | Florian J. G. Waleczek[1,3] | Jonas A. Haas[1] | Anselm A. Derda[1,3] | Kristina Sonnenschein[1,3] | Anika Gietz[1] | Susanne Neumüller[1] | Angelika Pfanne[1] | Oliver Beetz[4,5] | Michael Pflaum[2,6,7] | Bettina Wiegmann[2,6,7] | Yiangos Psaras[8] | Christopher Toepfer[8] | Robert Zweigerdt[9] | Ante Radocaj[10] | Theresia Kraft[10] | Andre Zeug[11] | Evgeni Ponimaskin[11] | Wilhelm Korte[2] | Alexander Horke[2] | Arjang Ruhparwar[2] | Maximilian Fuchs[1] | Ke Xiao[1] | Christian Bär[1,12] | Natalie Weber[1,13] | Thomas Thum[1]

Correspondence
Thomas Thum and Natalie Weber, Institute for Molecular and Therapeutic Strategies (IMTTS), Hannover Medical School, Carl-Neuberg-Str. 1, 30625 Hannover, Germany.
Email: thum.thomas@mh-hannover.de and weber.natalie@mh-hannover.de

Funding information
This work was supported by ERC Advance Grant to T. T. (REVERSE) and SFB1470 to T. T.; by Förderstiftung MHH, German Society of Cardiology Grant (DGK Forschungsstipendium), nextGENERATION Medical Scientist Program funded by Else Kröner-Fresenius Foundation (2022_EKMK.13) and internal HILF stipend of Hannover Medical School to N. W.; by PRACTIS-Clinician Scientist Program of Hannover Medical School, funded by the German Research Foundation (DFG, ME

Abstract

Background and Purpose: Mavacamten (MAVA) is a novel small molecule inhibitor of cardiac myosin, mitigating cardiomyocyte hypercontractility in patients with hypertrophic obstructive cardiomyopathy (HOCM). Despite its recent approval for clinical use, the transcriptional and functional impacts of MAVA remain not well understood. In this study we investigate the effects of MAVA across diverse cardiac models, including healthy female porcine cardiomyocytes and myocardial slices, human induced pluripotent stem cell-derived cardiomyocytes (hiPSC-CMs), cardiac organoids and living myocardial slices (LMSs) derived from patients with HOCM.

Experimental Approach: Long-term LMS culture facilitated continuous force measurements, while SarcTrack and MUSCLEMOTION analyses were used to evaluate contractility in cardiomyocytes and cardiac organoids. Transcriptome profiling of MAVA-treated HOCM hiPSC-CMs and HOCM LMSs allowed in-depth examination of gene expression signatures in response to MAVA treatment.

Abbreviations: BMCC, biomimetic cultivation chambers; hiPSC-CMs, human induced pluripotent stem cell-derived cardiomyocytes; hCO, human cardiac organoid; HCM, hypertrophic cardiomyopathy; HOCM, hypertrophic obstructive cardiomyopathy; IHM, interactive head motif; LMSs, living myocardial slices; LVOTO, left ventricular outflow tract obstruction; MAVA, mavacamten; PLVCMs, porcine left ventricular cardiomyocytes; SRX, super-relaxed state of the myosin head.

Kiselev, E.; Agyapong, W.; Weber, N. and Thum T. are first or last authors.

For affiliations refer to page 16

3696/3-1) to A. D.; and Wellcome Sir Henry Dale Fellowship (222567/Z/21/Z) to C. T.

Key Results: Across all models tested, MAVA demonstrated robust force inhibition. In primary disease models, MAVA showed little effect on time to peak or relaxation times and even reduced contraction and relaxation velocities. By contrast, in engineered human HOCM models, MAVA accelerated both contraction and relaxation, suggesting potential model-specific effects. Transcriptome analyses revealed that MAVA treatment not only influenced contraction regulation but also significantly altered cytoskeleton organization, muscle stretch response, and metabolic pathways. Notably, in LMSs derived from three HOCM patients, MAVA treatment up-regulated myosin binding protein H (*MyBPH*) expression, suggesting that MyBPH may also be involved in contraction regulation.

Conclusion and Implications: These data suggest that MAVA not only inhibits force within the sarcomere but also influences transcriptional pathways in model-specific manner.

KEYWORDS

cardiac organoids, cardiomyocytes, contractile function, hypertrophic cardiomyopathy (HCM), living myocardial slices (LMS), mavacamten

1 | INTRODUCTION

Hypertrophic cardiomyopathy (HCM) is the most frequently occurring inherited cardiac muscle disease, characterized by hypertrophy of the interventricular septum and left ventricular wall, fibrosis, and myocyte disarray. Patients often develop angina, heart failure, arrhythmias, and have a high risk for sudden cardiac death (Maron & Maron, 2013; Seidman & Seidman, 2011). About 50% of HCM cases involve mutations in sarcomeric protein genes such as *MYH7* (ventricular myosin heavy chain) and *MYBPC3* (cardiac myosin binding protein C) (Marian, 2021).

Classical heart failure drugs, including beta-blockers and calcium channel blockers, treat symptoms but do not target the underlying sarcomere dysfunction or halt hypertrophy and fibrosis progression. Recent research highlights the super-relaxed state (SRX) of myosin heads with low ATP turnover, which is disrupted by HCM mutations, causing hypercontractility (Anderson et al., 2018; Hooijman et al., 2011; Spudich et al., 2016).

Mavacamten (MAVA), a myosin inhibitor recently approved for obstructive HCM (HOCM), reduces hypercontractility by stabilizing the SRX state. It has shown efficacy in preclinical models by suppressing hypertrophy, reducing fibrosis-related gene expression, and improving relaxation (Green et al., 2016). Clinically, MAVA improves oxygen consumption, functional classification, and lowers left ventricular outflow tract obstruction (LVOTO) gradient in HOCM patients (EXPLORER-HCM [Olivotto et al., 2020]; PIONEER-HCM [Heitner et al., 2019]).

Various studies explored MAVA's effects in engineered and primary HOCM models, consistently showing decreased contractile force and improved relaxation (Sewanan et al., 2021; Sparrow et al., 2020; Toepfer et al., 2020). For example, MAVA treatment of engineered heart tissues results in reduced stiffness and relaxation time with preserved length-dependent contraction despite lower peak power (Sewanan et al., 2021). In cardiomyocytes with thin filament mutations, MAVA partially reversed increased calcium sensitivity and improved calcium handling (Green et al., 2016). However, patient-derived myocardial slices showed prolonged contraction and relaxation phases, extended refractory periods, and potential anti-arrhythmic effects (Amesz et al., 2023). Mechanistically, MAVA normalizes contractility by stabilizing myosin SRX and counteracting mutation-induced energetic stress (Nag et al., 2017; Spudich et al., 2016).

However, different model systems yield variable results. Mature adult cardiomyocytes reflect disease effects accurately but are difficult to maintain in vitro (Banyasz et al., 2008). Engineered hiPSC-derived cardiomyocytes (hiPSC-CMs) show immature phenotypes that

What is already known?

- Mavacamten is an inhibitor of cardiac myosin, reducing hypercontractility in HOCM.

What does this study add?

- Application of mavacamten to various cardiac model systems affects force, kinetics and transcriptome differentially.

What is the clinical significance?

- Cardiac models should be specifically selected for individual patients and mutations.

affect contractility and drug responses (Iorga et al., 2017; Weber et al., 2016; Yang et al., 2014). Single-cell models lack essential tissue interactions, limiting their ability to fully capture disease complexity. In contrast, multicellular models such as cardiac organoids (hCOs) and living myocardial slices (LMSs) provide a more comprehensive disease context—organoids replicate early-stage disease with multiple cell types, while LMS represent advanced disease characterized by native fibrotic remodelling (Fischer et al., 2019; Mohr et al., 2022; Richards et al., 2017).

This study compares MAVA's functional impacts across multiple HOCM models, including porcine and patient-derived LMSs, hiPSC-CMs and hCOs. We also investigate transcriptional changes induced by MAVA using RNA sequencing and gene set enrichment analysis in hiPSC-CMs and human LMSs.

2 | METHODS

2.1 | Animal experiments

Heart samples were obtained from healthy adult female German domestic pigs (average 40 kg). The experiments were approved by LAVES (Lower Saxony State Office for Consumer Protection and Food Safety) and conducted in accordance with EU guidelines and German animal protection laws. The animals were euthanized for reasons unrelated to this study using zoletil, atropine, narcofol and pentobarbital. The heart was quickly excised, transported in ice-cold Tyrode's solution and processed within 15 min. Animal studies are reported in compliance with the ARRIVE guidelines (Percie du Sert et al., 2020) and with the recommendations made by the *British Journal of Pharmacology* (Lilley et al., 2020).

2.2 | Human tissue

Myocardial tissue from patients with hypertrophic obstructive cardiomyopathy (HOCM) was obtained during myectomy surgery after approval by the Hannover Medical School ethics committee (No. 2997-2016) and informed consent, following the Declaration of Helsinki (World Medical Association declaration of Helsinki, 1997).

2.3 | Preparation of living myocardial slices (LMSs)

Heart tissue was embedded in low-melting agarose (Sigma-Aldrich, St. Louis, USA) and sliced at 300-µm thickness using a high-precision vibrating microtome (Model 7000SMZ-2, Campden Instruments, Loughborough, England), and kept in Tyrode's solution at 4°C. LMSs were randomly assigned to control or MAVA treated groups. LMSs designated for prolonged culture were trimmed to approximately 6.5 mm × 6.5 mm, aligned with muscle fibres and attached to plastic scaffolds (InVitroSys, Gräfelfing, Germany) or rings for force measurement.

2.4 | Ex vivo culture and contraction analysis

Myocardial slices from pigs and two HOCM patients were cultured in a biomimetic auxotonic system (InVitroSys, Gräfelfing, Germany) at 37°C with electrical stimulation (0.2 Hz). Contraction parameters were recorded over 96 and 72 h using the MyoDish system. Force data were normalized to baseline, and fold changes were calculated to assess drug effects.

2.5 | Primary cardiomyocyte isolation and sarcomere length measurement

Cardiomyocytes were isolated from LMSs using collagenase (Worthington Biochemical Corporation, Lakewood, USA) digestion, seeded on laminin-coated (Thermo Fisher, Waltham, USA) coverslips (Fisher Scientific, Pittsburgh, USA), and stimulated electrically. Sarcomere length and contraction velocities were measured via Fourier analysis with IonWizard software (IonOptix, Westwood, USA) (Mutig et al., 2013).

2.6 | hiPSC maintenance and differentiation

HOCM-R723G hiPSCs were cultured on Geltrex (Life Technologies, Carlsbad, USA) in mTeSR1 medium (Stemcell Technologies, Vancouver, Canada), differentiated into cardiomyocytes via Wnt pathway modulation and purified by metabolic selection (Foinquinos et al., 2020). Experiments were performed between Days 54 and 58 post-differentiation.

2.7 | Fabrication of human cardiac organoids (hCOs) and contractility measurement

Organoids were created using agarose molds (Merck, Darmstadt, Germany), combining 50% HOCM-hiPSC-derived cardiomyocytes with non-cardiomyocytes (fibroblasts, endothelial cells and adipose-derived stem cells). Cultured in ratiometric media with growth factors, they were treated with MAVA (Selleck Chemicals, Houston, USA; 0.3 µM) for 5 days. Contractility measurement was performed and analyzed using MUSCLEMOTION (Sala et al., 2018).

2.8 | MAVA treatment in various models

MAVA (0.3 µM) or DMSO (Roth, Karlsruhe, Germany; Control, 0.0014%) were applied to cardiomyocytes, LMS and organoids. Treatments ranged from acute to several days, with medium refreshed regularly.

2.9 | Contractility analysis in HOCM hiPSC-cardiomyocytes

AAV6 vectors carrying ACTN2-eGFP (Addgene, Waterntown, USA) were produced in HEK293T cells, purified via PEG (Roth,

Karlsruhe, Germany) precipitation and iodixanol (Progen, Heidelberg, Germany) ultracentrifugation, and used to transduce cardiomyocytes. Sarcomere contractions were measured using spinning disk confocal microscopy and sarcomere tracking analysis using Matlab-based SarcTrack (Toepfer et al., 2019).

2.10 | Molecular biology

RNA was isolated from tissue and cell samples, then used for quantitative PCR (qPCR) and RNA sequencing. Sequencing data were processed with nfcore/rnaseq, aligned to the reference genome and analysed using DESeq2 for differential gene expression analysis.

2.11 | Data and statistical analysis

Data were compared using paired or unpaired Student's t-test where applicable. *P*-values ≤ 0.05 were considered statistically significant. Detailed information on the performed statistical tests and the experimental numbers are included in the respective figure legends. Data and statistical analysis comply with the recommendations on experimental design and analysis in pharmacology (Curtis et al., 2025). For experiments where n<5, the results should be regarded as preliminary.

Detailed information on methods is provided in the supporting information.

2.12 | Nomenclature of targets and ligands

Key protein targets and ligands in this article are hyperlinked to corresponding entries in http://www.guidetopharmacology.org and are permanently archived in the Concise Guide to PHARMACOLOGY 2023/24 (Alexander, Christopoulos, et al., 2023; Alexander, Fabbro, et al., 2023).

3 | RESULTS

3.1 | MAVA reduces contractile amplitude and slows force kinetics in porcine myocardial slices and cardiomyocytes

Initially, to test how increasing MAVA concentrations affect the contractile properties of LMSs generated from healthy porcine left ventricular myocardium, we evaluated contractile force in the organ bath (Figure 1a). Increasing MAVA concentrations immediately reduced maximum force, with half maximal inhibitory concentration (IC_{50}) ranging from 0.2 to 0.7 μM, depending on the pig and preparation (Figures 1b and S1). Based on these experiments we decided to use 0.3 μM as the optimal dose for long-term application of MAVA in ex vivo and in vitro CM cultures. By increasing MAVA concentrations in multicellular pig LMS or in human HOCM hiPSC-CMs (Figure S2) we could not observe any signs of toxicity.

To determine if single cardiomyocyte measurement reflects the effect of MAVA on contractile parameters, we applied MAVA to porcine left ventricular cardiomyocytes (PLVCMs) isolated from freshly generated LMS (Figure 1c) and assessed sarcomere shortening parameters (Figure 1d–j). Representative recordings of sarcomere shortening in the same PLVCM before (grey) and after (red) MAVA treatment are shown in Figure 1d. Resting sarcomere length appears unaffected by MAVA treatment (Figure 1e). Contraction amplitude was significantly reduced as compared to control PLVCMs (Figure 1f). Time to peak of contraction and half relaxation time were highly variable in CMs derived from individual pig hearts, both in control and with MAVA treatment (Figure 1g,h). Nevertheless, MAVA decreased maximum contraction velocity and relaxation velocity (Figure 1i,j). Overall, these data indicate that MAVA alters sarcomere shortening in porcine cardiomyocytes.

3.2 | MAVA reduces force generation but has only minor effects on gene expression patterns in ex vivo culture of porcine myocardial slices

To investigate functional and gene expression effects of MAVA in a porcine multicellular preparation, we kept porcine LMS in biomimetic cultivation chambers (BMCC) with MAVA or control for 96 h and continuously recorded force generation. Figure 1k shows the ex vivo cultivation scheme in BMCC. During the first 24 h after MAVA administration, MAVA-treated wild-type porcine LMS had strongly reduced force compared to the control group throughout the entire cultivation period (Figure 1l). MAVA had negligible effects on time to peak and half relaxation time at any analysed time point (Figure 1m,n). At all timepoints, porcine LMS showed slower maximum contraction and relaxation velocities after MAVA treatment (Figure 1o,p). Overall, the data demonstrate that MAVA effectively lowers force generation in multicellular porcine wild-type LMS and leads to slow contraction and relaxation velocities.

MAVA treatment has been shown to decrease fibrosis- and hypertrophy-related gene expression in HCM mice (Green et al., 2016). Expression patterns in multicellular heart preparations have not been studied. The expression of genes regulating hypertrophy (*NPPA*), contractility (*MYH7*, *ATP2A2*) and fibrosis (*COL1A1*, *CCN2*) were not altered in porcine LMS after 96 hours of culture with or without added MAVA (Figure S3). Consistent with these findings, morphological structure was well preserved in both MAVA treated and control solution treated porcine LMS, and tissue collagen deposition as quantified by Picro Sirius Red staining did not change after MAVA treatment (Figure S3). To conclude, MAVA had only minor effects on gene expression levels, tissue morphology and collagen deposition in healthy porcine myocardial tissue, results that may indicate its mode of action is different in the context of HCM.

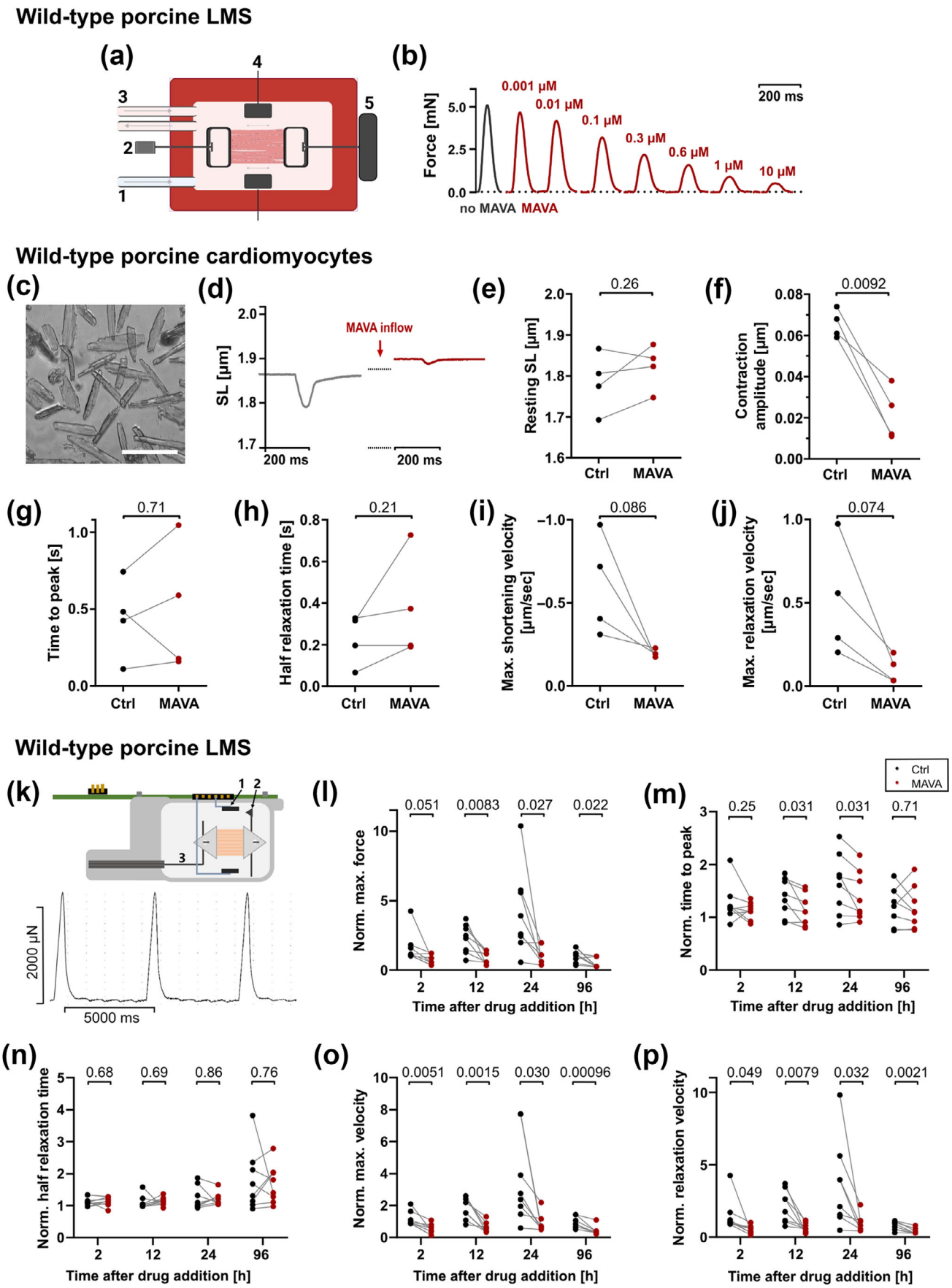

FIGURE 1 Legend on next page.

3.3 | MAVA regulates contractility and shortening kinetics in hiPSC-cardiomyocytes and human cardiac organoids with HOCM

To further translate our experimental findings to the human disease setting, we investigated the effects of MAVA on gene expression and CM function in human in vitro HOCM models. HiPSC were obtained from a HOCM patient with a R723G β-myosin heavy chain mutation and then differentiated into cardiomyocytes, as described previously (Merkert et al., 2021; Weber et al., 2025). HOCM hiPSC-CMs were transduced with AAV6-*ACTN2-EGFP* encoding sarcomeric α-actinin-2-EGFP to visualize sarcomeres in intact cardiomyocytes for contractility measurements, which were analysed by SarcTrack (Toepfer et al., 2019) (Figure 2a).

We assessed the effects of acute MAVA treatment on sarcomere shortening by initially detecting each cardiomyocyte under basal conditions (control) and then measuring the same cardiomyocyte after MAVA administration (Figure 2b). After acute MAVA application, resting sarcomere length in HOCM hiPSC-CMs significantly increased (Figure 2c) while contraction amplitude dropped significantly to 52% of baseline (Figure 2d). Time to peak was significantly shorter for MAVA-treated cardiomyocytes (Figure 2e), while relaxation time did not change (Figure 2f).

hCOs represent a flexible and high-throughput multicellular model system that bridges the low complexity of single cell type 2 D culture and high complexity but low throughput/availability of human HOCM LMS (Richards et al., 2017). Here, we generated HOCM hCOs by assembling 50% HOCM hiPSC-CMs with R723G myosin missense mutation (Weber et al., 2025) and 50% non-cardiomyocytes (cardiac fibroblasts, endothelial cells, mesenchymal stem cells), as described recently (Richards et al., 2017). The hCOs were treated with MAVA for 5 days and the contractile characteristics analysed by the MUSCLEMOTION ImageJ plug-in (Sala et al., 2018). A micrograph of an hCO and representative time traces of paced contractions in HOCM hCO with and without MAVA are shown in Figure 2g,h (for videos of a contracting control and MAVA hCOs, see Videos S1 and S2). In MAVA-treated HOCM hCOs, contraction amplitude and time to peak of contraction decreased significantly compared to control (Figure 2i,j). Interestingly, relaxation time was also reduced (Figure 2k), suggesting the multicellular engineered HOCM hCO model (R723G mutation) responds to MAVA differently than HOCM hiPSC-CMs (R723G mutation) in 2D cell culture. Moreover, we examined HOCM hCOs for gene expression changes in response to MAVA treatment with specific focus on hypertrophy-related (*NPPA*, *NPPB*), excitation–contraction-related (*MYH7/MYH6*, *APT2A2*) and fibrosis-associated (*COL1A1*, *CCN2*) gene expression (Figure 2l–q). We observed lower *NPPA* expression in the MAVA group (Figure 2l), while *MYH7/MYH6*, *ATP2A2* and fibrosis-associated genes were not significantly changed.

Overall, we found that MAVA application strongly regulates contractility in both in vitro human HOCM models, but MAVA's effects on relaxation kinetics appear to vary between simple and more complex disease models.

3.4 | MAVA reduces force generation and slows force kinetics in living myocardial slices (LMSs) derived from hypertrophic obstructive cardiomyopathy (HOCM) patients

LMSs can be generated from HOCM patients' hearts and can be assumed to recapitulate drug responses, for example to MAVA, similarly as in vivo. Here, we generated LMSs from septal myectomies from two HOCM patients, added MAVA or control solution and then cultivated them for 3 days in BMCC (Figure 3a). From the tissue of a third HOCM patient, we prepared miniaturized slices (mini-LMS) because the available tissue sample was small. The mini-LMSs were incubated with MAVA or control solution and used for RNA sequencing. The clinical data for all three HOCM patients showed a thickened intraventricular septum, LVOTO gradient and supra-normal left ventricular ejection fraction (Figure 3b). We had no access to the genetic information of these three patients. However, the classical HOCM phenotype would indicate MAVA treatment for these patients independent of the underlying genetic status. Histological staining with

FIGURE 1 Mavacamten (MAVA) reduces contractile amplitude and slows the kinetics of contraction and relaxation in porcine myocardial slices and isolated cardiomyocytes. (a) Scheme of isometric force measurement in the organ bath. Porcine living myocardial slices (LMSs) were stretched, electrically stimulated (0.2 Hz) and subjected to increasing MAVA-concentrations (no MAVA; MAVA 0.001, 0.01, 0.1, 0.3, 0.6, 1 and 10 μM), while maximum force was recorded. In the scheme the numbers indicate: *1* and *3*, inflow and outflow tubes for perfusion; *2*, adjustable-length wire to mechanically stretch the LMS; *4*, pacing electrodes and *5*, isometric force transducer. (b) Recordings of averaged force transients at increasing MAVA concentrations. (c) Rod-shaped isolated primary wild-type porcine cardiomyocytes. Scale bar: 100 μm. (d) Representative averaged sarcomere contraction of a porcine cardiomyocyte before MAVA exposure (grey) and 15 min after MAVA exposure (0.3 μM, red). (e) Sarcomere length in μm before stimulation; (f) contraction amplitude in μm; (g) time to peak of contraction in seconds; and (h) half relaxation time in seconds; (i) maximum shortening velocity in μm/s; and (j) maximum relaxation velocity in μm/s. In Panels (e)–(j), each data point represents the mean measured value from one pig heart, two to three coverslips per pig heart, with five to 16 measured cardiomyocytes per coverslip and per condition. (k) Top: schematic of the experimental setup with mounted LMSs (orange) in BMCC. LMSs were electrically stimulated using electrodes (1). Auxotonic force was registered using a magnetic sensor (2). Preload was applied by a wire (3). Bottom: representative contraction force recording. (l) Normalized force without MAVA application (Ctrl, black) and after application of 0.3 μM MAVA (red); (m) normalized time to peak of contraction; (n) normalized half relaxation time; (o) normalized maximum contraction velocity; and (p) normalized relaxation velocity 2, 12, 24 and 96 h after MAVA or control (Ctrl) application. Data were normalized to the mean before drug application (batch correction). In Panels (l)–(p) each data point represents the average measured value from one pig heart (n = 8 pig hearts with three LMS per pig heart). The number of LMS per pig heart was variable due to loss of contractility in some of the LMS. Statistical significance was tested using individual paired Student's *t* test. The numbers represent unadjusted *P* values.

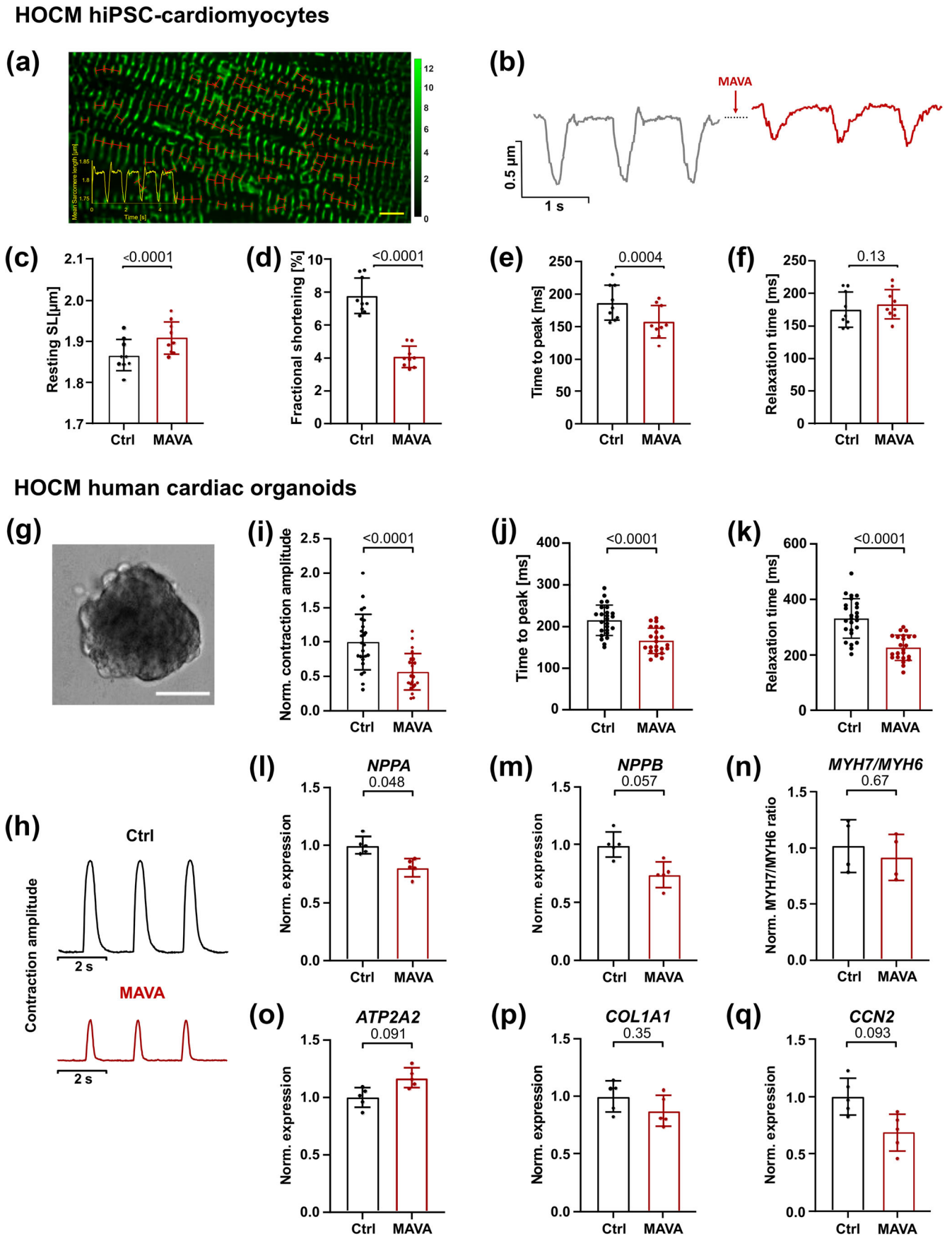

FIGURE 2 Legend on next page.

Picro Sirius Red demonstrated variable fibrotic remodelling of myocardium from the HOCM patients (Figure S4). MAVA or control solution treatments were administered starting on day one of the ex vivo culture. Example force recordings of HOCM LMS upon control solution or MAVA administration and averaged twitch forces at 2 h after drug administration, shown in Figure 3c,d, illustrate strongly reduced contractile force upon MAVA application. Overall, MAVA-treated HOCM LMS developed a significant ~70% decrease in force over 72-h culture as compared to control (Figure 3d,e), though the temporal parameters of force did not significantly differ between control and MAVA (Figure 3f,g). Additionally, both the maximum contraction and relaxation velocities of HOCM LMS were significantly lower with MAVA at 2 and 24 h after treatment (Figure 3h,i).

3.5 | MAVA regulates gene expression in HOCM hiPSC-CMs and living myocardial slices (LMSs) derived from hypertrophic obstructive cardiomyopathy (HOCM) patients

The activation of mechanosensing elements in the sarcomere is associated with regulation of downstream signalling pathways related to cardiac hypertrophy, cytoskeleton organization and sarcomere contraction (Knöll et al., 2003; Riaz et al., 2022). In preventive treatments, MAVA suppressed the activation of pro-hypertrophic and pro-fibrotic gene programs in HCM mice (Green et al., 2016). We therefore hypothesized that MAVA, could alter gene expression in addition to impacting contractile function in cardiomyocytes and myocardial slices.

We treated HOCM hiPSC-CMs from three independent differentiations from one patient line with R723G myosin missense mutation (Weber et al., 2025) with MAVA or control solution for 5 days and then performed RNA sequencing (Figure 4). In simple mode DESeq2 analysis we identified 1305 dysregulated genes (Figure 4a), 41 of which were changed significantly (fold-change >1.5, $P \leq 0.05$). The top 10 significantly up-regulated protein coding genes were: *SORCS1*, *COL25A1*, *CUBN*, *MGAT4C*, *TMEM155*, *RMDN2*, *VCAM1*, *LPRC7*, *GDPD2* and *SCN3A*. The top 10 significantly down-regulated protein coding genes were: *NANOS1*, *ADGRL4*, *TNFRSF12A*, *HBEGF*, *JUN*, *C5AR1*, *PDLIM3*, *FSTL3*, *ARID5A* and *NPPB* (Figure 4b). Enrichment analysis with GO biological process (GOBP) indicated regulated pathways not only for muscle contraction but also for cytoskeleton and sarcomere organization, protein phosphorylation, the **epidermal growth factor receptor** signalling pathway, glycolytic processes and cardiac action potential and calcium homeostasis (Figures 4c and S5). Interestingly, MAVA impacted the expression of *PDLIM* and *CSRP* transcript isoforms, which are known to be involved in regulating mechanosensing and hypertrophy-related signalling in sarcomeres, suggesting that MAVA has effects beyond force regulation in HOCM hiPSC-CMs.

To analyse MAVA effects on expression patterns in an ex vivo patient-derived HOCM model, we performed RNA sequencing of MAVA treated or control solution treated HOCM LMSs from three different HOCM patients with unknown HOCM genotypes (Figure 5). In simple mode DESeq2 analysis we identified 905 genes (Figure 5a). Among these, 395 genes were significantly changed (fold-change >1.5, $P \leq 0.05$). The top 10 significantly up-regulated protein coding genes were: *MYBPH*, *GCNT3*, *MYOT*, *POU6F2*, *SLC24A2*, *CMKLR2*, *RAB33A*, *VSX1*, *ZDHHC2* and *MLXIPL*. The top 10 significantly down-regulated protein coding genes were *RHOH*, *CLDN14*, *GPR78*, *NGFR*, *DNAH9*, *NPIPB13*, *CHEK1*, *SLX1B*, *NXF3* and *TTC22* (Figure 5b). Enriched categories in GOBP show that, similar to in HOCM hiPSC-CMs, MAVA treatment in HOCM LMS regulated not only the expression of genes involved in the contractile function of the myocardium but also of genes involved in cytoskeleton organization, protein catabolism, glucose homeostasis, cellular calcium ion transport homeostasis, ion transmembrane transport, fibroblast growth factor receptor signalling pathway and vascular smooth muscle cell migration (Figures 5c and S6). However, between the individual HOCM patients, gene regulations in response to MAVA were heterogeneous except for *MYBPH* which was significantly up-regulated in all three patients (Figure 5d).

Next, we investigated if the in vitro 2D HOCM hiPSC-CMs model (R723G myosin mutation) (Weber et al., 2025) and ex vivo 3D HOCM LMS model have comparable transcriptional responses. We identified

FIGURE 2 Mavacamten (MAVA) reduces contractility and accelerates contractile kinetics in hypertrophic obstructive cardiomyopathy (HOCM) hiPSC-CMs and HOCM hCOs with R723G myosin mutation. (a) HOCM hiPSC-CMs with R723G myosin missense mutation were transduced with AAV6-*ACTN2-eGFP* and sarcomere function was measured in control (Ctrl) medium (grey: time trace of contraction) and after MAVA addition in the same cardiomyocyte (b; MAVA 0.3 μM; red: time trace). Red bars: video-tracked sarcomeres. Scale on the right side: fluorescence intensity. Scale bar: 5 μm. SarcTrack (Toepfer et al., 2019) was used to evaluate contractile parameters: (c) Sarcomere length in micrometres before electrical stimulation for HOCM-hiPSC CMs before (black) and after (red) MAVA application. (d) Contraction amplitude in % of initial sarcomere length. (e) Time to peak in milliseconds. (f) Relaxation time in milliseconds. Data from three independent differentiations of the R723G cell line, three dishes per differentiation, 6–21 cardiomyocytes per dish. Each dot represents the mean for the cardiomyocytes per dish. Bars represent mean ± SD. Significance was tested using paired Student's *t* test. (g) HOCM-hCO with R723G myosin missense mutation (typical micrograph, scale bar: 100 μm). HOCM-hCOs were treated with MAVA (0.3 μM) or Ctrl for 5 days. Contraction videos were acquired at 37°C and 0.5-Hz pacing. (h) Original contraction time trace of a HOCM-hCO. Parameters were analysed using MUSCLEMOTION (Sala et al., 2018). (i) Normalized contraction amplitude (values are normalized to all Ctrl hCOs), black: Ctrl, red: MAVA. (j) Time to peak in milliseconds. (k) Relaxation time in milliseconds; 23–25 HOCM-hCOs per condition. Each dot represents one hCO. Gene expressions normalized to housekeeper gene expression and Ctrl (batch correction) of (l) *NPPA*, (m) *NPPB*, (n) *MYH7*/*MYH6* ratio, (o) *ATP2A2*, (p) *COL1A1* and (q) *CCN2*. In Panels (l)–(q) each data point represents the mean of hCOs harvested from one independent differentiation (n = 5 differentiations). In Panel (n) *MYH6* was not analysable for one of the differentiations. Therefore only four values are shown. Bars represent mean ± SD. Significance was tested using unpaired (i–k) and paired (l–q) Student's *t* test.

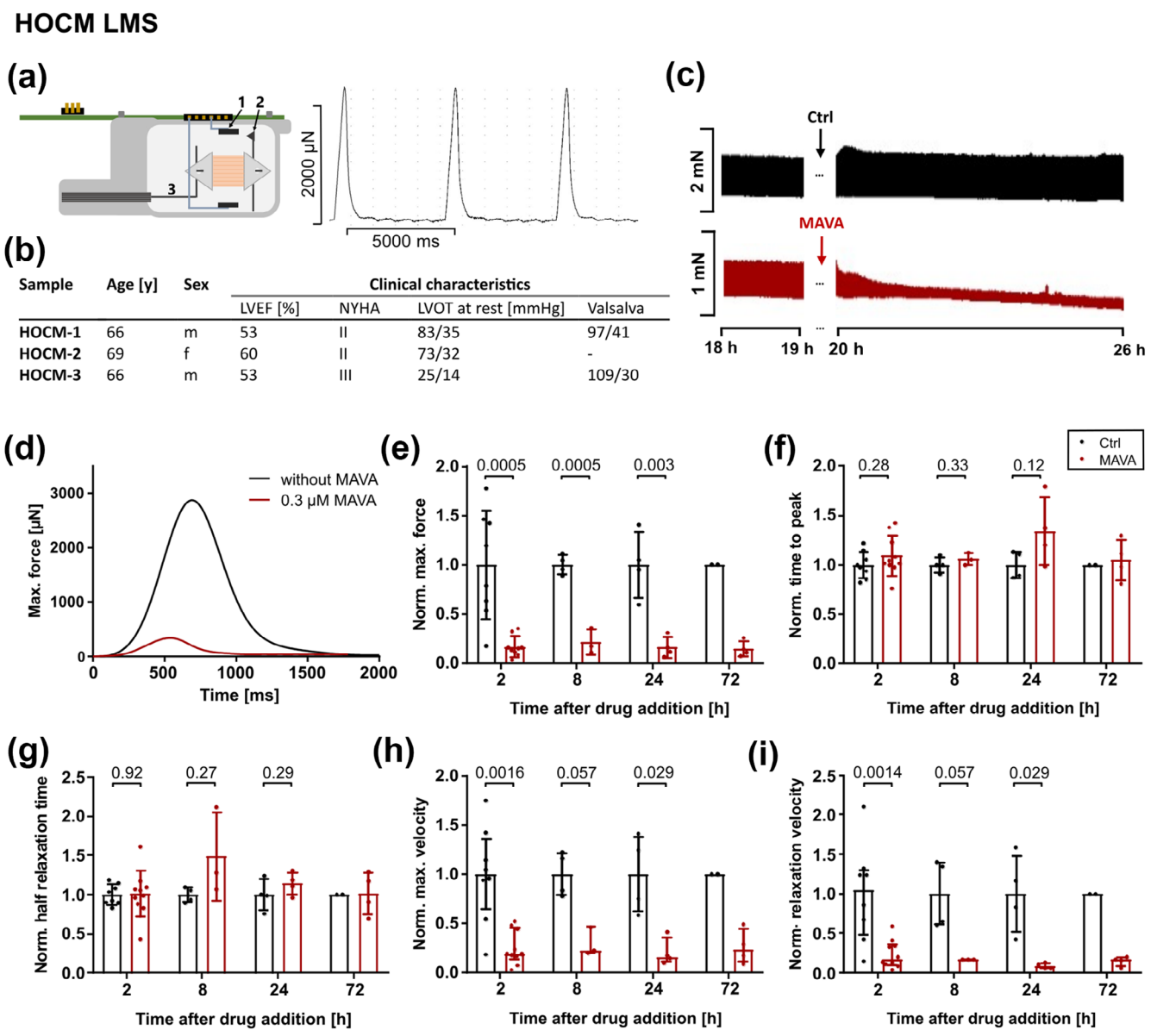

Sample	Age [y]	Sex	Clinical characteristics			
			LVEF [%]	NYHA	LVOT at rest [mmHg]	Valsalva
HOCM-1	66	m	53	II	83/35	97/41
HOCM-2	69	f	60	II	73/32	-
HOCM-3	66	m	53	III	25/14	109/30

FIGURE 3 Effects of mavacamten (MAVA) on contraction amplitude and contraction and relaxation kinetics in hypertrophic obstructive cardiomyopathy (HOCM) living myocardial slices (LMSs). (a) Experimental setup and recording as in Figure 1k; (b) clinical data from three HOCM patients. LVEF: left ventricular ejection fraction in %; IVSED: end-diastolic thickness of interventricular septum in mm; LVOTO: left ventricular outflow tract obstruction gradient in mmHg (first number indicates maximum pressure gradient, second number indicates mean pressure gradient); NYHA: heart failure classification. In Patient 1, the provoked gradient under Valsalva was 97/41 mmHg. In Patient 2, a Valsalva manoeuvre could not be performed; however, the diagnosis and therapeutic indication were already confirmed by a resting gradient of >50 mmHg. LVOTO under Valsalva was 109/30 mmHg in Patient 3, as reported in the external findings based on which the patient was referred to HTTG. This indicates that the patient was also eligible for mavacamten therapy. (c) Representative recordings of MAVA- and Ctrl-treated human HOCM LMS under 18 to 26 h of ex vivo culture and (d) at 2 h after drug addition. (e) Normalized maximum force; (f) normalized time to peak; (g) normalized half relaxation time; (h) normalized maximum contraction velocity; and (i) normalized maximum relaxation velocity of HOCM LMS after Ctrl treatment (black) and after addition of 0.3 µM MAVA (red) at 2, 8, 24 and 72 h of ex vivo culture. Each data point represents the measured value for one LMS. The response to the electrical stimulation of the LMS decreased drastically over time, leaving many LMS unanalyzable at later time points. Therefore, the sample size decreased from 2 to 72 h. LMS prepared from two HOCM patients, two to three LMS per patient and per condition. Contractile parameters were normalized to baseline of the Ctrl group. Bars represent mean ± SD (e–g) or median ± interquartile range (h,i). As n=3 for these experiments, statistical analysis was not carried out, and results should be regarded as preliminary.

25 overlapping genes in HOCM hiPSC-CMs and HOCM LMS, and MAVA treatment up-regulated 14 genes and down-regulated 11 genes in both disease models (Figure 6a, Table S2). Since patient-derived HOCM hiPSC-CMs from one HOCM patient harbouring the R723G myosin mutation were utilized in this study, we asked if MAVA regulates gene expression similarly in samples from different HOCM

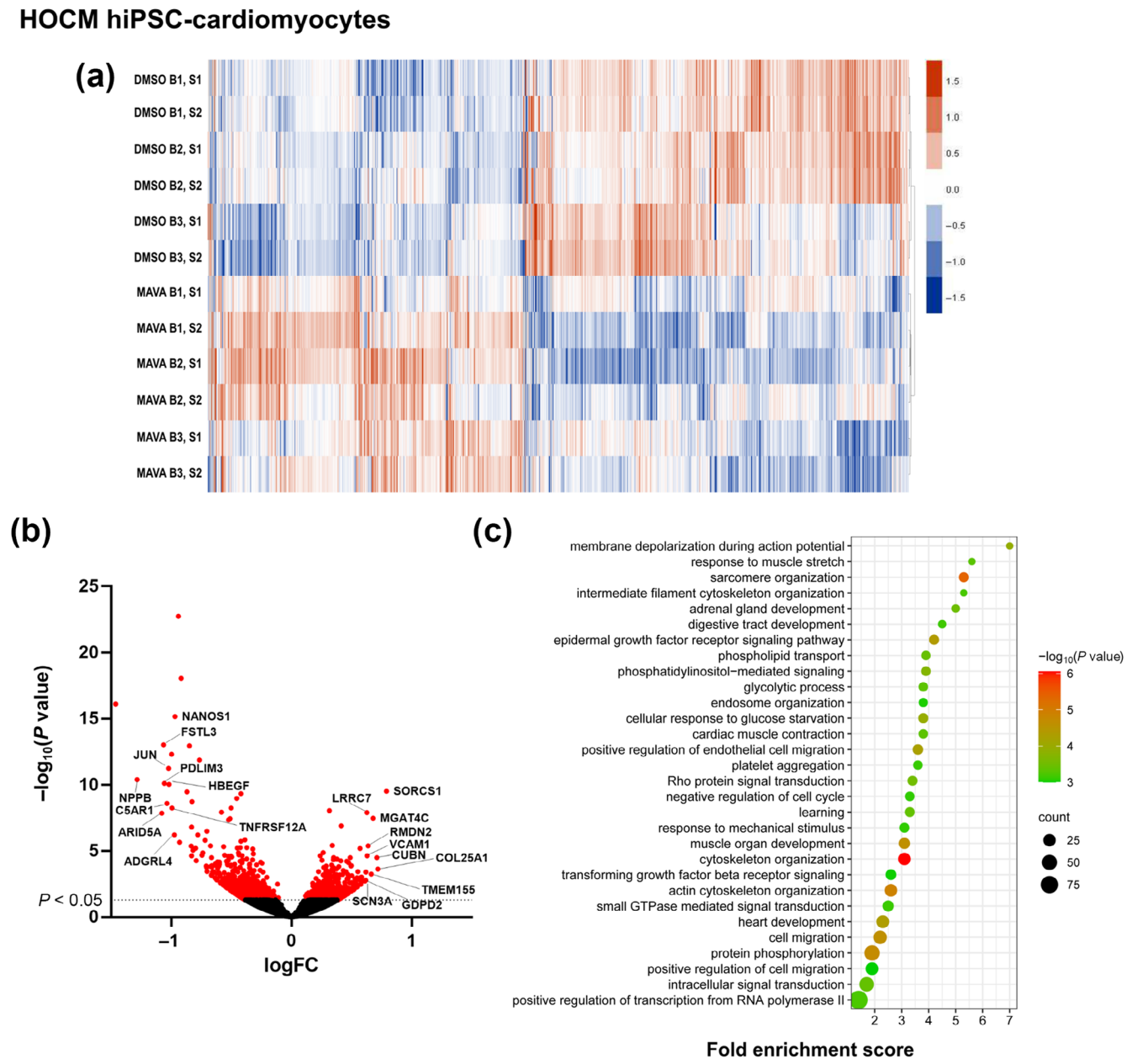

FIGURE 4 Mavacamten (MAVA)-induced changes in gene expression in hypertrophic obstructive cardiomyopathy (HOCM) hiPSC-cardiomyocytes with R723G myosin mutation. (a) Heatmap of 1305 genes regulated by MAVA treatment, as determined by default (one factor) DESeq2 analysis ($P < 0.05$). Genes up-regulated by MAVA are indicated in red, genes down-regulated in blue. We produced three differentiations (B1, B2 and B3) which we treated with DMSO (control) and with MAVA, and measured two wells for each differentiation and treatment (indicated by S1 and S2). (b) Volcano plot of all 18,478 detected genes. The 1305 differentially expressed genes were significantly changed ($P < 0.05$) and are indicated in red above the horizontal line ($P \leq 0.05$). The top 10 most up- and down-regulated genes (based on fold-change) are annotated in the plot. (c) Top 30 GO biological process enriched by 1305 dysregulated genes ($P < 0.05$). Bubble plot representing the enriched GOBP pathways. *X* axis: fold enrichment score. For the heatmap and volcano plot, raw read counts from all samples were analyzed using Deseq2 under default settings. The *P*-values were obtained based on wald test and corrected by Benjamini and Hochberg method according to the Deseq2 manual. Gene list ($P < 0.05$) derived after Deseq2 process were analyzed further using DAVID web server for functional annotation and enrichment analysis. Fold enrichment score is a ratio comparing the percentage of a functional Term in our list versus its percentage in target database. P-values were based on Fisher's Exact test adopted by DAVID.

patients. We therefore investigated how MAVA treatment altered expression in LMSs from three different HOCM patients. Apart from sharing the general HOCM phenotype (Figure 3b), the myocardium from all three patients displayed highly variable histological phenotypes and degrees of fibrosis (Figure S6), findings that suggest differential states of cardiac tissue remodelling. There were 119 overlapping genes that reacted to MAVA treatment in all three HOCM patients, but only eight genes were regulated in the same manner for

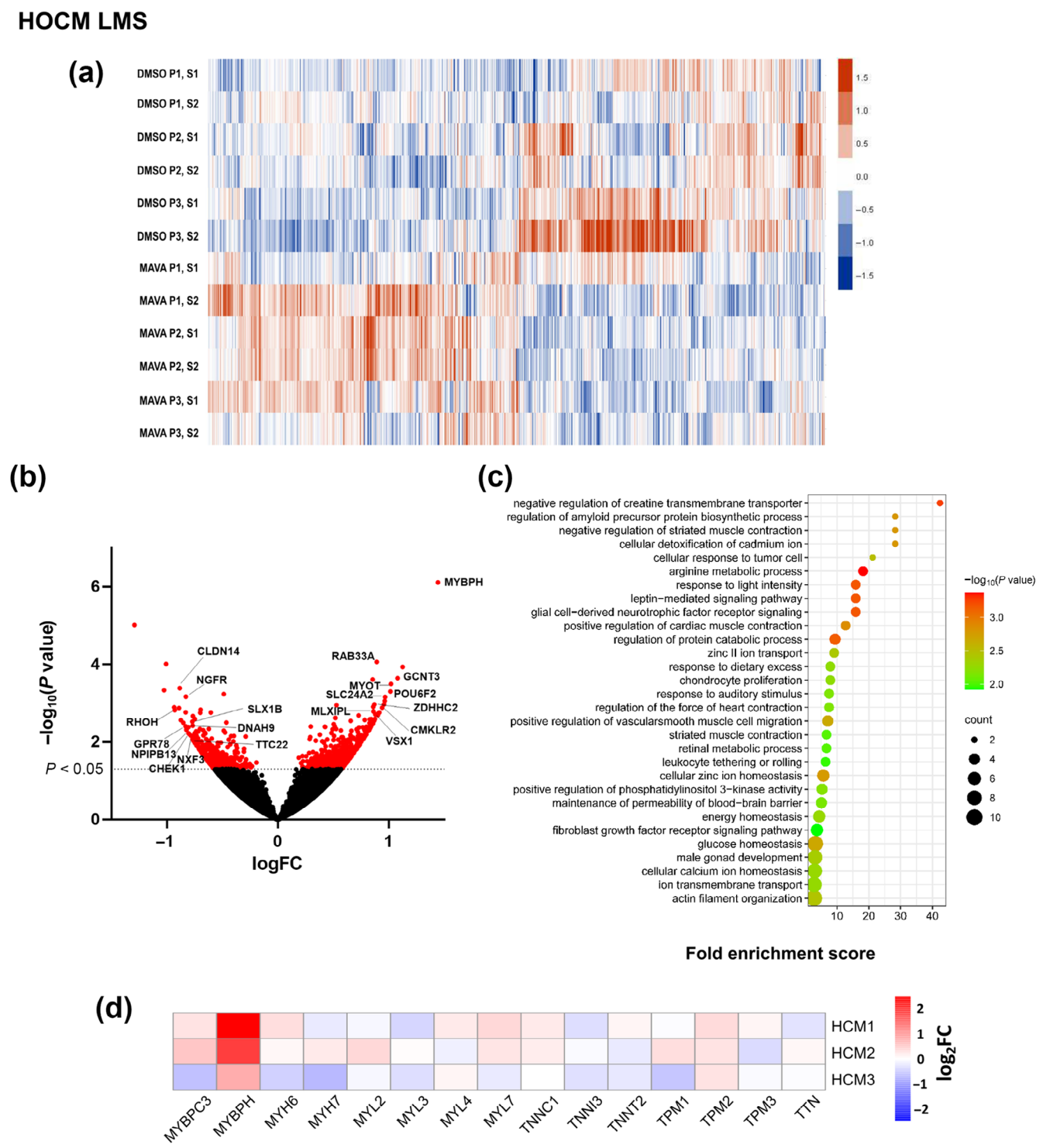

FIGURE 5 Mavacamten (MAVA) treatment changes gene expression in hypertrophic obstructive cardiomyopathy (HOCM) living myocardial slices (LMSs). (a). Heatmap of 395 genes in human HOCM LMSs, with MAVA-regulated genes ($P < 0.05$) determined by default (one factor) DESeq2 analysis. Upregulated genes are indicated in red and downregulated genes are indicated in blue. Each column represents one LMS from one of three HOCM patients (P1–P3) after Ctrl or MAVA treatment. (b) Volcano plot of all 28,564 detected genes. The 890 differentially expressed genes were significantly changed ($P < 0.05$) and are indicated in red above the horizontal line ($P \leq 0.05$). The top 10 most up and downregulated genes (based on fold-change) are annotated in the plot. (c) Top 30 GO biological process enriched by 905 deregulated genes ($P < 0.05$). Bubble plot representing the enriched GOBP pathways. *X* axis: fold enrichment score. (d). Heatmap of differential expression of sarcomere genes for the individual HCM patients (HCM-1 to HCM-3). Colour code is indicating $\log_2$ (fold change) of mRNA expression for MAVA-treated versus control treated LMS. Note that dysregulation was only significant for *MYBPH* gene. For each of the three patients the expression of this gene was upregulated, while other sarcomere genes showed variable expression in each patient. As n=3 for these experiments, results should be regarded as preliminary.

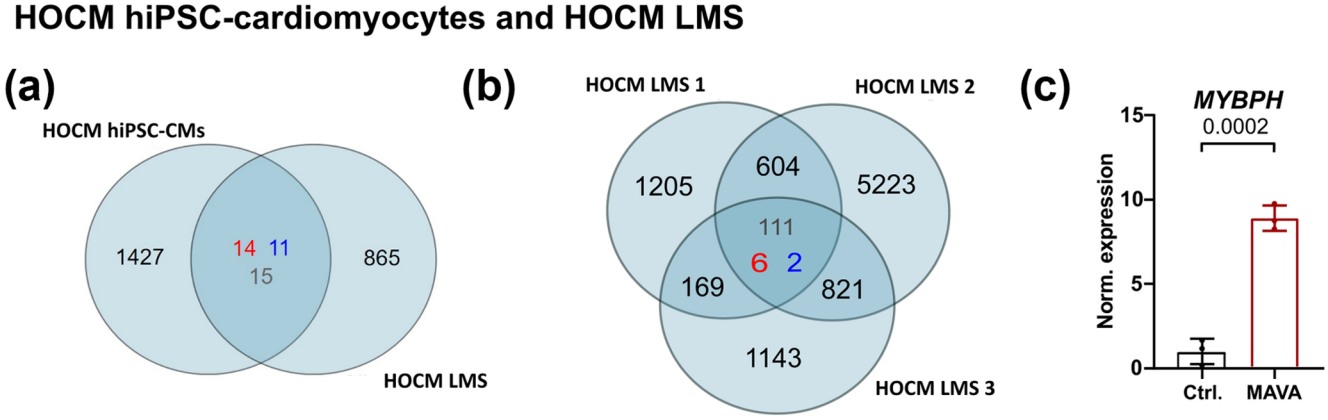

(d)

Elements	Base mean	log2(FC)	P-value	Gene symbol
ENSG00000132763.15	527.34	0.68	0.017	*MMACHC*
ENSG00000123106.11	1906.09	0.53	0.0011	*CCDC91*
ENSG00000140297.13	38.45	1.08	0.00022	*GCNT3*
ENSG00000108846.16	9715.56	0.86	0.00025	*ABCC3*
ENSG00000162496.9	908.23	0.77	0.0082	*DHRS3*
ENSG00000133055.10	320.32	1.44	7.8E-7	*MYBPH*
ENSG00000064300.9	1523.44	-0.83	0.00068	*NGFR*
ENSG00000110876.10	421.46	-0.63	0.026	*SELPLG*

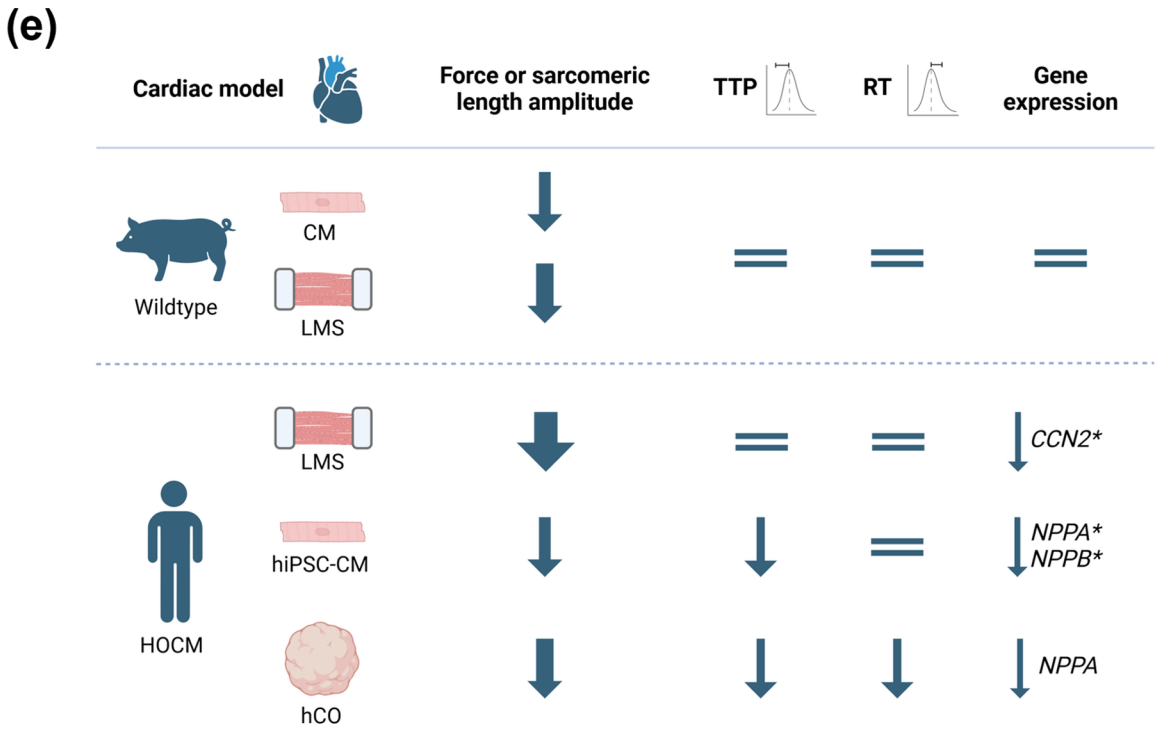

FIGURE 6 Legend on next page.

all three HOCM patients, with six genes up-regulated and two genes down-regulated after MAVA treatment (Figure 6b,d). Most interestingly, one of the consistently up-regulated genes, confirmed by qPCR analysis ($P \leq 0.001$), was myosin binding protein H (*MYBPH*), a known modulator of cardiac muscle contraction (Mouton et al., 2015) (Figure 6c). *MYBPH* has been associated with the hypertrophic phenotype in HCM (Mouton et al., 2016) and therefore may play a role in contraction regulation after MAVA treatment and possibly in the therapeutic mechanism of MAVA in HOCM.

To provide a comprehensive overview of our findings, Figure 6e summarizes the differential effects of MAVA across the various disease models used. This includes its influence on contractile function in both engineered hiPSC-CM systems and native HOCM myocardium, as well as its modulation of disease-relevant transcriptional pathways. The schematic highlights both shared and model-specific responses, emphasizing the importance of CM maturity and disease stage.

4 | DISCUSSION

MAVA, a novel drug developed to target HOCM, has recently garnered attention for its influence on cardiomyocyte contractile force and kinetics through direct inhibition of myosin. Our study aimed to compare MAVA treatment responses in various primary and engineered single cell and multicellular cardiac healthy and HOCM models. Decreased force generation after MAVA treatment was a consistent outcome across all the models. However, there were substantial differences in the effect of MAVA on the contractile kinetics between primary and engineered models.

We used porcine myocardium due to its physiological similarity to the human heart including comparable cardiac structure, function and contractile properties. Additionally, the ready availability of porcine LMS ensured reproducibility and reliability of our experiments and helped us to determine the dose response range for MAVA prior to investigations in human HOCM models.

The effects of MAVA on force reduction and contractile kinetics in porcine healthy LMS were similar to the functional effects of MAVA in human HOCM LMS, even though the porcine healthy LMS showed lesser reduction in generated force with MAVA than human HOCM LMS. This could be due to the fact that human HOCM LMS showed strong tissue remodelling that presumably reduced the amount of the myofilaments per cross-sectional area, so that the applied effective concentration of MAVA per myofilament could be higher. However, possible HOCM mutations, which we have not investigated in this study, could also explain different reactions of human HOCM LMSs to MAVA as compared to healthy porcine LMSs. In both these primary models MAVA slowed down the contraction and relaxation kinetics. It has been observed that MAVA reduces the number of myosin heads available for force production (Anderson et al., 2018). However, this by itself cannot explain the reduction in relaxation velocity which we observed in primary cardiac models.

Because of the limited availability of human HOCM LMSs as a highly translational model it is favourable to use patient-derived human iPSC-(hiPSC)-CM models. Single-cell hiPSC-derived cultures, though, do not include possible cross-talk between different cardiac cell types within a three-dimensional environment. Cardiac organoids bridge the gap between 2D cell cultures and complex in-vivo models. They enable high-throughput disease modelling with human-derived tissue, capturing cell interactions.

In both single cell and multicellular HOCM hiPSC-CM models, we observed reduced fractional shortening and altered sarcomere kinetics with MAVA treatment. Yet, the specific effects differed between the models, potentially because of different mechanical loads (more isotonic versus more isometric contractions) on the cardiomyocytes and different cellular interactions. Moreover, we cannot exclude that different experimental conditions, for example, media composition, pacing rate and other conditions could contribute to some degree to the distinct effects of MAVA observed here. However, each experiment consisted of the control samples exposed to the exactly same conditions as MAVA-treated samples allowing to conclude about MAVA effects for each model system. Moreover, the here used experimental conditions are state-of-the art for culture and functional measurements for the different model systems.

Comparing the HOCM hiPSC-CM models to the primary HOCM disease model we found that the contraction and relaxation kinetics were faster in the HOCM hiPSC-CM models with MAVA. The isoforms of the sarcomeric proteins could be differently expressed in engineered and primary myocardium (Iorga et al., 2017; Weber et al., 2016) and the cellular compositions with extracellular matrix could differ between the models, influencing the kinetics. In contrast to the hiPSC-CM based models, which imitate the early disease stage, the HOCM LMS model consists of native myocardium with the respective disease-specific

FIGURE 6 Mavacamten (MAVA) regulates *MyBPH* expression in living myocardial slices (LMSs) of hypertrophic obstructive cardiomyopathy (HOCM) patients. (a) Illustration of genes regulated in the same manner between MAVA-treated group and control (Ctrl) group (red = upregulated, blue = downregulated) of HOCM hiPSC-CMs (three independent differentiations) and HOCM LMSs (from three individual HOCM patients), as well as genes regulated in the opposite manner (grey). (b) Genes regulated in the same manner among HOCM LMSs, prepared from three different HOCM patients (HOCM LMS-1-3), treated with MAVA or Ctrl. RNA expressions that were up-regulated (red) or down-regulated (blue) in the same manner or regulated in the opposite manner (grey) between three individual HOCM LMS preparations. (c) qPCR analysis of *MyBPH* gene expression in HOCM LMS treated with MAVA or Ctrl. Each dot represents the average of both samples/condition for each HOCM patient. Gene expression results were normalized to the reference gene HPRT and to the means of the Ctrl group ($2^{-\Delta\Delta Ct}$ method, batch correction). (d) List of genes regulated in the same manner between MAVA-treated group and Ctrl in HOCM LMS from three individual patients, with Ensembl ID, base mean, log2 fold-change, *P* value and gene symbol. (e) Summary of functional and expressional effects of MAVA in the different cardiac models. Arrow thickness represents effect size, and an equality sign indicates no significant effects. Expression was analysed by RT-qPCR or RNA-seq*. As n=3 for these experiments, results should be regarded as preliminary.

changes in all present cell types and excessive collagen deposition representing an advanced stage of the disease.

The faster contraction and relaxation kinetics observed in engineered HOCM hiPSC-CM models compared to primary native myocardium can be attributed to several key factors.

Firstly, hiPSC-CMs represent an immature developmental stage, often expressing sarcomeric protein isoforms distinct from adult myocardium. Engineered models tend to express the fast cardiac myosin heavy chain isoform, whereas mature adult myocardium predominantly expresses the slow myosin heavy chain isoform. Additionally, engineered tissues usually show low cardiac troponin I expression, with a relative predominance of the skeletal troponin I isoform, all contributing to accelerated contractile kinetics.

Second, the cellular and extracellular environment differs markedly. Primary HOCM myocardium contains diverse native cell types—all carrying the diseased phenotype—and a complex extracellular matrix with fibrosis, imposing mechanical constraints that slow contraction and relaxation. In contrast, engineered models mostly contain only diseased cardiomyocytes, with other cell types being healthy or absent, and lack significant fibrosis, leading to faster kinetics.

Finally, primary myocardium reflects an advanced disease stage with chronic remodelling, while hiPSC-CM models typically mimic early-stage disease without these adaptations, further explaining the kinetic differences.

Together, developmental immaturity, distinct sarcomeric isoform expression, simplified cellular composition, and disease progression stage underlie the divergence in contractile behaviour between engineered and native HOCM models.

MAVA directly targets the sarcomere by inhibiting hypercontractile myosin heads, thereby providing a cell-specific modulation of contractility based on the degree of myosin dysregulation in individual cardiomyocytes. In contrast, β-blockers act upstream by blocking **β-adrenoceptors**, leading to a more generalized reduction in contractile activity through modulation of the excitation-contraction coupling pathway, assuming similar receptor density and intracellular signalling among cells. Because MAVA acts directly at the sarcomere level, it offers a more precise and targeted mechanism of action for HOCM, potentially reducing hypercontractility with fewer systemic effects. This targeted approach may complement or offer advantages over β-blockers in managing hypercontractility in HOCM patients, highlighting the translational potential of MAVA as a novel therapeutic strategy.

In all models MAVA alters sarcomere contraction. Altered mechanosensation leads to changes in the activation of downstream signalling pathways involved in hypertrophy and fibrosis (Knöll et al., 2003; Riaz et al., 2022). By inhibiting the myosin ATPase MAVA reduces ATP consumption and could affect the transcriptional regulation of metabolic pathways. This mechanism can be pronounced by varying degrees in different model systems. In HOCM hiPSC-CMs with R723G myosin missense mutation treated with MAVA, we detected regulation of gene expressions not only in the pathways of muscle contraction, actin cytoskeleton organization, and muscle stretch response, but also of protein phosphorylation, glycolytic processes, cardiac action potential and calcium homeostasis. This indicates that MAVA effects reach beyond the regulation of force production in cardiomyocytes. Among the top 10 significantly down-regulated genes we identified *NPPB* and *PDLIM3*. *NPPB* is the classical marker of myocyte hypertrophy and heart failure (Fu et al., 2018). Its down-regulation indicates attenuation of hypertrophy with MAVA. *PDLIM3* codes for the actin-associated LIM protein, which is localized in the Z-disc of the sarcomere and is involved in crosslinking of actin filaments and force transmission. Mutations in PDLIM genes are associated with HCM development (Zheng et al., 2022). Additionally, MAVA-induced changes in the expression of genes for key proteins in the Z-disc, for example, *CSRP3*, *FHL2* and *LIMK1*. These proteins are known to be involved in the mechanosensation of the sarcomere and pro-hypertrophic signalling (Linke, 2008).

Similarly, in HOCM patient-derived LMS, expression of genes related to muscle contraction, energy metabolism and cellular signalling pathways were regulated with MAVA. Surprisingly, we found a large heterogeneity among the patients with only six genes commonly regulated. This presumably reflects the heterogeneity of the underlying HCM mutation, sex, medication and comorbidities which were undisclosed. Nevertheless, among the differentially expressed genes, myosin binding protein H (*MYBPH*) was strongly up-regulated.

Myosin Binding Protein H (MyBPH) is encoded by a single gene (*MYBPH*) and expressed in both fast skeletal and cardiac muscle cells, including Purkinje fibres (Mouton et al., 2015). It localizes specifically to stripe 3 within the C-zone (counting from the M-line) in predominantly fast-twitch muscle fibres (Mead et al., 2024). Structurally, MyBPH shares considerable similarity with cMyBPC, both being multi-domain proteins composed of immunoglobulin (Ig) like and **fibronectin type III** (FnIII) like domains. Both proteins are known to bind myosin, suggesting overlapping or complementary roles in thick filament regulation (Irving, 2017).

Given these structural and functional parallels, we propose that MyBPH may play a significant role in the organization and function of the cardiac sarcomere. However, its precise role remains largely unexplored, particularly in the context of cardiac muscle physiology and pathology. The observed up-regulation of MyBPH following MAVA treatment in HOCM patient-derived myocardium suggests that it might contribute to sarcomere remodelling or stabilization in response to therapeutic modulation of contractility. Understanding how MyBPH interacts with myosin and other sarcomeric proteins could provide valuable insights into its potential role in maintaining sarcomere integrity and modulating contractile dynamics under both physiological and disease conditions.

Differences in the transcriptional regulations to MAVA in both human in vitro and ex vivo models could be due to the different HOCM-associated genetical status of these models. While the HOCM-hiPSC-cardiomyocytes with R723G myosin mutation had a clear HOCM causing genotype (Enjuto et al., 2000; Weber et al., 2025), the samples from three individual HOCM-hearts were not further genetically characterized. These differences could explain potential mutation-specific functional and different transcriptional regulations in both models. However, the severe HOCM-phenotype of the three HOCM-patients would probably meet the criteria for therapeutical MAVA application, providing the rationale for investigating MAVA effects in our study.

However, our model systems cannot capture three-dimensional dynamic phenomena of the whole organ, such as LVOTO. Furthermore, investigations of the relationship between the functional and transcriptional effects of MAVA in in vitro and ex vivo models with characterized HOCM-associated mutations could be useful.

4.1 | Limitations of the study

A limitation of our study is the small number of HOCM patient myocardial samples (n = 2 for functional data and n = 3 for sequencing data), which restricts the ability to perform systematic comparisons of clinical characteristics or treatment responses. While we provide detailed clinical information in the Supplementary Materials, the limited sample size precludes definitive conclusions about patient-specific variability. Nonetheless, analysis of disease-relevant gene expression profiles from RNA-seq data reveals distinct individual transcriptional responses to MAVA, reflecting each patient's unique clinical history and disease background. These findings highlight the complexity of HOCM and underscore the need for larger patient cohorts to validate and extend these observations.

We assessed force generation and sarcomere shortening in various in vitro and ex vivo cardiac models to evaluate the functional impact of MAVA. Although MAVA reduced both force generation and sarcomere shortening amplitude across all models, the contractile kinetics were affected differently in primary versus engineered cardiac models. These differences in response may be attributed to variations in the maturity of cardiomyocytes, as well as experimental factors such as pacing rate, medium composition and the mechanical load on the cardiomyocytes. Additionally, differences in the cellular and extracellular matrix compositions, along with cellular interactions, between multicellular disease models at early (HOCM-hCOs) and advanced disease stages (HOCM-LMS), may further explain the divergent MAVA responses, highlighting the need for deeper investigation in future studies.

Moreover, the lack of information regarding the genotype of the HOCM-LMS limits our understanding of how MAVA might interact with specific HOCM mutations, which could provide valuable insight into its effects. While we identified transcriptional changes in cytoskeleton organization and Z-disc mechanosensing induced by MAVA, further research is necessary to determine the relevance of these changes to the functional response of cardiac tissue to MAVA.

4.2 | Translational perspective

MAVA is a novel myosin inhibitor applied to ameliorate contractile dysfunction in patients with HOCM, the most frequent inherited heart disease. However, the drug's effects across different cardiac model systems have not been thoroughly investigated. To facilitate effective bench-to-bedside translation and further research into MAVA's mechanisms of action, a comprehensive comparison of its effects across various model systems is essential. In this study, we compared both functional and transcriptional responses to MAVA in multiple porcine and human primary and engineered HOCM models to gain a deeper understanding of its mode of action. Our findings revealed that in all models, force and contraction were reduced to varying extents, while the effects on kinetics and gene expression differed. These results underscore the importance of model selection in evaluating the drug's effects.

Effective drug concentration could be different in treated patients than in our study. In the PIONEER-HCM study a target therapeutic range of 350–700 ng/ml plasma concentration of MAVA was identified (Heitner et al., 2019). This corresponds to a MAVA concentration of 1.28–2.56 μM in patient's plasma. However the concentration in the muscle tissue is considered to be lower due to plasma protein binding resulting in estimated 0.04–0.08 μM (Prescribing Information for Camzyos, n.d.). We applied MAVA concentration of 0.3 μM based on the measured IC_{50} value. We assume that effects of MAVA are less pronounced in patients than in our study.

The models applied in this study offer complementary insights into MAVA's effects at different disease stages. The question remains which of the models or possibly combination of models are representative for the clinical use. Integrating data from early-stage engineered hiPSC-CMs and advanced primary myocardium can help tailor treatments to individual patient profiles, supporting more precise and effective application.

For the first time, we also examined the effects of MAVA on transcriptional regulation in patient-derived LMSs with HOCM. Our findings reveal that MAVA influences transcriptional networks, suggesting its impact extends beyond mere force inhibition. Further research is warranted to explore these effects in patients receiving MAVA treatment.

5 | CONCLUSIONS

Altogether, our findings demonstrate that in primary and engineered cardiac models some functional parameters are regulated differently with MAVA and that MAVA not only affects the kinetics of contractility, but also mechanosensation-related transcriptional pathways. Consequently, depending on the applied cardiac model, MAVA operates differentially on function and gene expression. This has to be considered in the planning of future research on myosin-modifying drugs. But also, a possible influence of MAVA on transcriptional pathways has to be examined for the effective treatment of HOCM patients.

AUTHOR CONTRIBUTIONS

Elisa Kiselev: Investigation (lead); writing—original draft (equal). **Wilson Agyapong:** Investigation (equal); writing—review and editing (equal). **Bjarne Jürgens:** Formal analysis (equal); investigation (supporting). **Elisa Mohr:** Formal analysis (equal); investigation (supporting). **Shambhabi Chatterjee:** Resources (equal); writing—review and editing (equal). **Hannah J. Hunkler:** Resources (equal). **Jawad Salman:** Resources (supporting). **Giuseppe Cipriano:** Formal analysis (equal); visualization (supporting); writing—review and editing (equal). **Marco**

Bentele: Formal analysis (equal); investigation (supporting); writing—review and editing (equal). **Junqing Liu:** Investigation (equal). **Jonas Specht:** Investigation (supporting). **Kaja S. Menge:** Investigation (equal). **Florian J. G. Waleczek:** Formal analysis (equal); visualization (equal). **Jonas A. Haas:** Investigation (supporting). **Anselm A. Derda:** Resources (equal). **Kristina Sonnenschein:** Resources (supporting). **Anika Gietz:** Resources (equal). **Susanne Neumüller:** Investigation (equal). **Angelika Pfanne:** Investigation (equal). **Oliver Beetz:** Resources (supporting). **Michael Pflaum:** Resources (supporting). **Bettina Wiegmann:** Resources (supporting). **Yiangos Psaras:** Software (equal). **Christopher Toepfer:** Software (equal). **Robert Zweigerdt:** Resources (supporting). **Ante Radocaj:** Writing—review and editing (supporting). **Theresia Kraft:** Resources (supporting). **Andre Zeug:** Formal analysis (equal); resources (equal). **Evgeni Ponimaskin:** Resources (equal). **Wilhelm Korte:** Resources (equal). **Alexander Horke:** Resources (equal); writing—review and editing (equal). **Arjang Ruhparwar:** Resources (equal). **Maximilian Fuchs:** Formal analysis (equal). **Ke Xiao:** Formal analysis (equal). **Christian Bär:** Resources (supporting). **Natalie Weber:** Conceptualization (equal); data curation (equal); funding acquisition (equal); project administration (equal); writing—original draft (equal); writing—review and editing (equal). **Thomas Thum:** Conceptualization (equal); funding acquisition (equal); writing—review and editing (equal).

AFFILIATIONS

[1]Institute of Molecular and Translational Therapeutic Strategies (IMTTS), Hannover Medical School, Hannover, Germany
[2]Department of Cardiothoracic, Transplantation and Vascular Surgery, Hannover Medical School, Hannover, Germany
[3]Department of Cardiology and Angiology, Hannover Medical School, Hannover, Germany
[4]Department of General, Visceral and Transplant Surgery, Hannover Medical School, Hannover, Germany
[5]Department of General, Visceral, Pediatric and Transplantation Surgery, University Hospital RWTH Aachen, Aachen, Germany
[6]Lower Saxony Center for Biomedical Engineering, Implant Research and Development, Hannover Medical School, Hannover, Germany
[7]German Center for Lung Research, BREATH, Hannover Medical School, Hannover, Germany
[8]Cardiovascular Medicine, Radcliffe Department of Medicine (C.N.T.), University of Oxford, Oxford, UK
[9]Leibniz Research Laboratories for Biotechnology and Artificial Organs (LEBAO), Department of Cardiothoracic, Transplantation and Vascular Surgery, Hannover Medical School, Hannover, Germany
[10]Institute of Molecular and Cell Physiology, Hannover Medical School, Hannover, Germany
[11]Institute for Neurophysiology, Hannover Medical School, Hannover, Germany
[12]Fraunhofer Institute of Toxicology and Experimental Medicine (ITEM), Germany
[13]Dean's Office for Academic Career Development, next GENERATION Medical Scientist Program, Hannover Medical School, Hannover, Germany

ACKNOWLEDGEMENTS

We thank the patients and their families for kindly donating skin fibroblasts for generation of stem cell-derived cardiomyocytes and heart tissue for generation of LMS. We acknowledge the MHH research core facility for transcriptomics at Hannover Medical School and the Department of Device Construction (Gerätebau) at Hannover Medical School. Open Access funding enabled and organized by Projekt DEAL.

CONFLICT OF INTEREST STATEMENT

T. T. is the founder and CSO/CMO of Cardior Pharmaceuticals, a wholly-owned subsidiary of Novo Nordisk A/S Europe (not related to this study). T. T. filed and received royalties from patents about non-coding RNAs (not related to this study). A. D. received honoraria for lectures from AstraZeneca, BMS, Lilly and Bayer (not related to this study). All other authors declare no conflicts of interest.

DATA AVAILABILITY STATEMENT

The data that support the findings of this study are available from the corresponding author upon reasonable request. Some data may not be made available because of privacy or ethical restrictions.

DECLARATION OF TRANSPARENCY AND SCIENTIFIC RIGOUR

This Declaration acknowledges that this paper adheres to the principles for transparent reporting and scientific rigour of preclinical research as stated in the BJP guidelines for Natural Products Research, Design and Analysis, Immunoblotting and Immunochemistry and Animal Experimentation, and as recommended by funding agencies, publishers and other organizations engaged with supporting research.

REFERENCES

Alexander, S. P. H., Christopoulos, A., Davenport, A. P., Kelly, E., Mathie, A. A., Peters, J. A., Veale, E. L., Armstrong, J. F., Faccenda, E., Harding, S. D., Davies, J. A., Abbracchio, M. P., Abraham, G., Agoulnik, A., Alexander, W., Al-Hosaini, K., Bäck, M., Baker, J. G., Barnes, N. M., … Ye, R. D. (2023). The Concise Guide to PHARMACOLOGY 2023/24: G protein-coupled receptors. *Br J Pharmacol*, *180*, S23–S144. https://doi.org/10.1111/bph.16177

Alexander, S. P. H., Fabbro, D., Kelly, E., Mathie, A. A., Peters, J. A., Veale, E. L., Armstrong, J. F., Faccenda, E., Harding, S. D., Davies, J. A., Beuve, A., Brouckaert, P., Bryant, C., Burnett, J. C., Farndale, R. W., Friebe, A., Garthwaite, J., Hobbs, A. J., Jarvis, G. E., … Stasch, J. P. (2023). Waldman SA (2023a). The Concise Guide to PHARMACOLOGY 2023/24: Catalytic receptors. *Br J Pharmacol*, *180*, S241–S288. https://doi.org/10.1111/bph.161

Amesz, J. H., Langmuur, S. J. J., Epskamp, N., Bogers, A. J. J. C., de Groot, N. M. S., Manintveld, O. C., & Taverne, Y. J. H. J. (2023). Acute biomechanical effects of empagliflozin on living isolated human heart failure myocardium. *Cardiovascular Drugs and Therapy*, *38*, 659–666. https://doi.org/10.1007/s10557-023-07434-3

Anderson, R. L., Trivedi, D. V., Sarkar, S. S., Henze, M., Ma, W., Gong, H., Rogers, C. S., Gorham, J. M., Wong, F. L., Morck, M. M., Seidman, J. G., Ruppel, K. M., Irving, T. C., Cooke, R., Green, E. M., & Spudich, J. A. (2018). Deciphering the super relaxed state of human β-cardiac myosin and the mode of action of mavacamten from myosin molecules to muscle fibers. *Proceedings of the National Academy of Sciences of the*

United States of America, *115*, E8143–e8152. https://doi.org/10.1073/pnas.1809540115

Banyasz, T., Lozinskiy, I., Payne, C. E., Edelmann, S., Norton, B., Chen, B., Chen-Izu, Y., Izu, L. T., & Balke, C. W. (2008). Transformation of adult rat cardiac myocytes in primary culture. *Experimental Physiology*, *93*, 370–382. https://doi.org/10.1113/expphysiol.2007.040659

Curtis, M. J., Alexander, S. P. H., Cortese-Krott, M., Kendall, D. A., Martemyanov, K. A., Mauro, C., Panettieri, R. A. Jr., Papapetropoulos, A., Patel, H. H., Santo, E. E., Schulz, R., Stefanska, B., Stephens, G. J., Teixeira, M. M., Vergnolle, N., Wang, X., & Ferdinandy, P. (2025 Apr). Guidance on the planning and reporting of experimental design and analysis. *Br J Pharmacol.*, *182*(7), 1413–1415. https://doi.org/10.1111/bph.17441

Enjuto, M., Francino, A., Navarro-Lopez, F., Viles, D., Paré, J. C., & Ballesta, A. M. (2000). Malignant hypertrophic cardiomyopathy caused by the Arg723Gly mutation in beta-myosin heavy chain gene. *Journal of Molecular and Cellular Cardiology*, *32*, 2307–2313. https://doi.org/10.1006/jmcc.2000.1260

Fischer, C., Milting, H., Fein, E., Reiser, E., Lu, K., Seidel, T., Schinner, C., Schwarzmayr, T., Schramm, R., Tomasi, R., Husse, B., Cao-Ehlker, X., Pohl, U., & Dendorfer, A. (2019). Long-term functional and structural preservation of precision-cut human myocardium under continuous electromechanical stimulation in vitro. *Nature Communications*, *10*, 117. https://doi.org/10.1038/s41467-018-08003-1

Foinquinos, A., Batkai, S., Genschel, C., Viereck, J., Rump, S., Gyöngyösi, M., Traxler, D., Riesenhuber, M., Spannbauer, A., Lukovic, D., Weber, N., Zlabinger, K., Hašimbegović, E., Winkler, J., Fiedler, J., Dangwal, S., Fischer, M., de la Roche, J., Wojciechowski, D., … Thum, T. (2020). Preclinical development of a miR-132 inhibitor for heart failure treatment. *Nature Communications*, *11*, 633. https://doi.org/10.1038/s41467-020-14349-2

Fu, S., Ping, P., Wang, F., & Luo, L. (2018). Synthesis, secretion, function, metabolism and application of natriuretic peptides in heart failure. *Journal of Biological Engineering*, *12*, 2. https://doi.org/10.1186/s13036-017-0093-0

Green, E. M., Wakimoto, H., Anderson, R. L., Evanchik, M. J., Gorham, J. M., Harrison, B. C., Henze, M., Kawas, R., Oslob, J. D., Rodriguez, H. M., Song, Y., Wan, W., Leinwand, L. A., Spudich, J. A., McDowell, R. S., Seidman, J. G., & Seidman, C. E. (2016). A small-molecule inhibitor of sarcomere contractility suppresses hypertrophic cardiomyopathy in mice. *Science*, *351*, 617–621. https://doi.org/10.1126/science.aad3456

Heitner, S. B., Jacoby, D., Lester, S. J., Owens, A., Wang, A., Zhang, D., Lambing, J., Lee, J., Semigran, M., & Sehnert, A. J. (2019). Mavacamten treatment for obstructive hypertrophic cardiomyopathy: A clinical trial. *Annals of Internal Medicine*, *170*, 741–748. https://doi.org/10.7326/M18-3016

Hooijman, P., Stewart, M. A., & Cooke, R. (2011). A new state of cardiac myosin with very slow ATP turnover: a potential cardioprotective mechanism in the heart. *Biophysical Journal*, *100*, 1969–1976. https://doi.org/10.1016/j.bpj.2011.02.061

Iorga, B., Schwanke, K., Weber, N., Wendland, M., Greten, S., Piep, B., Dos Remedios, C. G., Martin, U., Zweigerdt, R., Kraft, T., & Brenner, B. (2017). Differences in contractile function of myofibrils within human embryonic stem cell-derived cardiomyocytes vs. adult ventricular myofibrils are related to distinct sarcomeric protein isoforms. *Frontiers in Physiology*, *8*, 1111.

Irving, M. (2017). Regulation of Contraction by the Thick Filaments in Skeletal Muscle. *Biophysical Journal*, *113*, 2579–2594. https://doi.org/10.1016/j.bpj.2017.09.037

Knöll, R., Hoshijima, M., & Chien, K. (2003). Cardiac mechanotransduction and implications for heart disease. *Journal of Molecular Medicine (Berlin, Germany)*, *81*, 750–756.

Lilley, E., Stanford, S. C., Kendall, D. E., Alexander, S. P. H., Cirino, G., Docherty, J. R., George, C. H., Insel, P. A., Izzo, A. A., Ji, Y., Panettieri, R. A., Sobey, C. G., Stefanska, B., Stephens, G., Teixeira, M., & Ahluwalia, A. (2020). ARRIVE 2.0 and the British Journal of Pharmacology: Updated guidance for 2020. *British Journal of Pharmacology*, *177*, 3611–3616. https://doi.org/10.1111/bph.15178

Linke, W. A. (2008). Sense and stretchability: The role of titin and titin-associated proteins in myocardial stress-sensing and mechanical dysfunction. *Cardiovascular Research*, *77*, 637–648.

Marian, A. J. (2021). Molecular Genetic Basis of Hypertrophic Cardiomyopathy. *Circulation Research*, *128*, 1533–1553. https://doi.org/10.1161/CIRCRESAHA.121.318346

Maron, B. J., & Maron, M. S. (2013). Hypertrophic cardiomyopathy. *Lancet*, *381*, 242–255. https://doi.org/10.1016/S0140-6736(12)60397-3

Mead, A. F., Wood, N. B., Nelson, S. R., Palmer, B. M., Yang, L., Previs, S. B., Ploysangngam, A., Kennedy, G. G., McAdow, J. F., Tremble, S. M., Zimmermann, M. A., Cipolla, M. J., Ebert, A. M., Johnson, A. N., Gurnett, C. A., Previs, M. J., & Warshaw, D. M. (2024). Functional role of myosin-binding protein H in thick filaments of developing vertebrate fast-twitch skeletal muscle. *Journal of General Physiology*, *156*, e202413604. https://doi.org/10.1085/jgp.202413604

Merkert, S., Wunderlich, S., Beier, J., Franke, A., Schwanke, K., Göhring, G., Kraft, T., Francino, A., Zweigerdt, R., & Martin, U. (2021). Generation of two iPSC clones (MHHi021-A and MHHi021-B) from a patient with hypertrophic cardiomyopathy with p.Arg723Gly mutation in the MYH7 gene. *Stem Cell Research*, *52*, 102208. https://doi.org/10.1016/j.scr.2021.102208

Mohr, E., Thum, T., & Bär, C. (2022). Accelerating cardiovascular research: Recent advances in translational 2D and 3D heart models. *European Journal of Heart Failure*, *24*, 1778–1791. https://doi.org/10.1002/ejhf.2631

Mouton, J., Loos, B., Moolman-Smook, J. C., & Kinnear, C. J. (2015). Ascribing novel functions to the sarcomeric protein, myosin binding protein H (MyBPH) in cardiac sarcomere contraction. *Experimental Cell Research*, *331*, 338–351. https://doi.org/10.1016/j.yexcr.2014.11.006

Mouton, J. M., van der Merwe, L., Goosen, A., Revera, M., Brink, P. A., Moolman-Smook, J. C., & Kinnear, C. (2016). MYBPH acts as modifier of cardiac hypertrophy in hypertrophic cardiomyopathy (HCM) patients. *Human Genetics*, *135*, 477–483. https://doi.org/10.1007/s00439-016-1649-7

Mutig, N., Geers-Knoerr, C., Piep, B., Pahuja, A., Vogt, P. M., Brenner, B., Niederbichler, A. D., & Kraft, T. (2013). Lipoteichoic acid from Staphylococcus aureus directly affects cardiomyocyte contractility and calcium transients. *Molecular Immunology*, *56*, 720–728. https://doi.org/10.1016/j.molimm.2013.07.007

Nag, S., Trivedi, D. V., Sarkar, S. S., Adhikari, A. S., Sunitha, M. S., Sutton, S., Ruppel, K. M., & Spudich, J. A. (2017). The myosin mesa and the basis of hypercontractility caused by hypertrophic cardiomyopathy mutations. *Nature Structural & Molecular Biology*, *24*, 525–533. https://doi.org/10.1038/nsmb.3408

Olivotto, I., Oreziak, A., Barriales-Villa, R., Abraham, T. P., Masri, A., Garcia-Pavia, P., Saberi, S., Lakdawala, N. K., Wheeler, M. T., Owens, A., Kubanek, M., Wojakowski, W., Jensen, M. K., Gimeno-Blanes, J., Afshar, K., Myers, J., Hegde, S. M., Solomon, S. D., Sehnert, A. J., … Yamani, M. (2020). Mavacamten for treatment of symptomatic obstructive hypertrophic cardiomyopathy (EXPLORER-HCM): a randomised, double-blind, placebo-controlled, phase 3 trial. *Lancet*, *396*, 759–769. https://doi.org/10.1016/S0140-6736(20)31792-X

Percie du Sert, N., Hurst, V., Ahluwalia, A., Alam, S., Avey, M. T., Baker, M., Browne, W. J., Clark, A., Cuthill, I. C., Dirnagl, U., Emerson, M., Garner, P., Holgate, S. T., Howells, D. W., Karp, N. A., Lazic, S. E., Lidster, K., MacCallum, C. J., Macleod, M., … Würbel, H. (2020). The ARRIVE guidelines 2.0: Updated guidelines for reporting animal research. *PLoS Biology*, *18*(7), e3000410. https://doi.org/10.1371/journal.pbio.3000410

Prescribing Information for Camzyos. (n.d.). Retrieved September 10, 2025, from https://www.accessdata.fda.gov/drugsatfda_docs/label/2022/214998s000lbl.pdf

Riaz, M., Park, J., Sewanan, L. R., Ren, Y., Schwan, J., das, S. K., Pomianowski, P. T., Huang, Y., Ellis, M. W., Luo, J., Liu, J., Song, L., Chen, I. P., Qiu, C., Yazawa, M., Tellides, G., Hwa, J., Young, L. H., Yang, L., … Qyang, Y. (2022). Muscle LIM Protein Force-Sensing Mediates Sarcomeric Biomechanical Signaling in Human Familial Hypertrophic Cardiomyopathy. *Circulation*, *145*, 1238–1253. https://doi.org/10.1161/CIRCULATIONAHA.121.056265

Richards, D. J., Coyle, R. C., Tan, Y., Jia, J., Wong, K., Toomer, K., Menick, D. R., & Mei, Y. (2017). Inspiration from heart development: Biomimetic development of functional human cardiac organoids. *Biomaterials*, *142*, 112–123. https://doi.org/10.1016/j.biomaterials.2017.07.021

Sala, L., van Meer, B. J., Tertoolen, L. G. J., Bakkers, J., Bellin, M., Davis, R. P., Denning, C., Dieben, M. A. E., Eschenhagen, T., Giacomelli, E., Grandela, C., Hansen, A., Holman, E. R., Jongbloed, M. R. M., Kamel, S. M., Koopman, C. D., Lachaud, Q., Mannhardt, I., Mol, M. P. H., … Mummery, C. L. (2018). MUSCLEMOTION: A Versatile Open Software Tool to Quantify Cardiomyocyte and Cardiac Muscle Contraction In Vitro and In Vivo. *Circulation Research*, *122*, e5–e16. https://doi.org/10.1161/CIRCRESAHA.117.312067

Seidman, C. E., & Seidman, J. G. (2011). Identifying sarcomere gene mutations in hypertrophic cardiomyopathy: a personal history. *Circulation Research*, *108*, 743–750. https://doi.org/10.1161/CIRCRESAHA.110.223834

Sewanan, L. R., Shen, S., & Campbell, S. G. (2021). Mavacamten preserves length-dependent contractility and improves diastolic function in human engineered heart tissue. *American Journal of Physiology. Heart and Circulatory Physiology*, *320*, H1112–h1123. https://doi.org/10.1152/ajpheart.00325.2020

Sparrow, A. J., Watkins, H., Daniels, M. J., Redwood, C., & Robinson, P. (2020). Mavacamten rescues increased myofilament calcium sensitivity and dysregulation of Ca(2+) flux caused by thin filament hypertrophic cardiomyopathy mutations. *American Journal of Physiology. Heart and Circulatory Physiology*, *318*, H715–h722. https://doi.org/10.1152/ajpheart.00023.2020

Spudich, J. A., Aksel, T., Bartholomew, S. R., Nag, S., Kawana, M., Yu, E. C., Sarkar, S. S., Sung, J., Sommese, R. F., Sutton, S., Cho, C., Adhikari, A. S., Taylor, R., Liu, C., Trivedi, D., & Ruppel, K. M. (2016). Effects of hypertrophic and dilated cardiomyopathy mutations on power output by human β-cardiac myosin. *The Journal of Experimental Biology*, *219*, 161–167. https://doi.org/10.1242/jeb.125930

Toepfer, C. N., Garfinkel, A. C., Venturini, G., Wakimoto, H., Repetti, G., Alamo, L., Sharma, A., Agarwal, R., Ewoldt, J. K., Cloonan, P., Letendre, J., Lun, M., Olivotto, I., Colan, S., Ashley, E., Jacoby, D., Michels, M., Redwood, C. S., Watkins, H. C., … Seidman, C. E. (2020). Myosin Sequestration Regulates Sarcomere Function, Cardiomyocyte Energetics, and Metabolism, Informing the Pathogenesis of Hypertrophic Cardiomyopathy. *Circulation*, *141*, 828–842. https://doi.org/10.1161/CIRCULATIONAHA.119.042339

Toepfer, C. N., Sharma, A., Cicconet, M., Garfinkel, A. C., Mücke, M., Neyazi, M., Willcox, J. A. L., Agarwal, R., Schmid, M., Rao, J., Ewoldt, J., Pourquié, O., Chopra, A., Chen, C. S., Seidman, J. G., & Seidman, C. E. (2019). SarcTrack. *Circulation Research*, *124*, 1172–1183. https://doi.org/10.1161/CIRCRESAHA.118.314505

Weber, N., Montag, J., Kowalski, K., Iorga, B., de la Roche, J., Holler, T., Wojciechowski, D., Wendland, M., Radocaj, A., Mayer, A. K., Brunkhorst, A., Osten, F., Burkart, V., Piep, B., Bodenschatz, A., Gibron, P., Schwanke, K., Franke, A., Thiemann, S., … Kraft, T. (2025). Patient-specific hiPSC-derived cardiomyocytes indicate allelic and contractile imbalance as pathogenic factor in early-stage Hypertrophic Cardiomyopathy. *Journal of Molecular and Cellular Cardiology*, *198*, 112–125. https://doi.org/10.1016/j.yjmcc.2024.11.007

Weber, N., Schwanke, K., Greten, S., Wendland, M., Iorga, B., Fischer, M., Geers-Knörr, C., Hegermann, J., Wrede, C., Fiedler, J., Kempf, H., Franke, A., Piep, B., Pfanne, A., Thum, T., Martin, U., Brenner, B., Zweigerdt, R., & Kraft, T. (2016). Stiff matrix induces switch to pure beta-cardiac myosin heavy chain expression in human ESC-derived cardiomyocytes. *Basic Research in Cardiology*, *111*, 68.

World Medical Association declaration of Helsinki. (1997). Recommendations guiding physicians in biomedical research involving human subjects. *Journal of the American Medical Association*, *277*, 925–926.

Yang, X., Pabon, L., & Murry, C. E. (2014). Engineering adolescence: maturation of human pluripotent stem cell-derived cardiomyocytes. *Circulation Research*, *114*, 511–523. https://doi.org/10.1161/CIRCRESAHA.114.300558

Zheng, J., Huang, Z., Hou, S., Jiang, X., Zhang, Y., Liu, W., Jia, J., Li, Y., Sun, X., Xie, L., Zhao, X., Hou, C., & Xiao, T. (2022). Case Report: Novel LIM domain-binding protein 3 (LDB3) mutations associated with hypertrophic cardiomyopathy family. *Frontiers in Pediatrics*, *10*, 947963. https://doi.org/10.3389/fped.2022.947963

SUPPORTING INFORMATION

Additional supporting information can be found online in the Supporting Information section at the end of this article.

How to cite this article: Kiselev, E., Agyapong, W., Jürgens, B., Mohr, E., Chatterjee, S., Hunkler, H. J., Salman, J., Cipriano, G., Bentele, M., Liu, J., Specht, J., Menge, K. S., Waleczek, F. J. G., Haas, J. A., Derda, A. A., Sonnenschein, K., Gietz, A., Neumüller, S., Pfanne, A., … Thum, T. (2025). Transcriptional and functional effects of mavacamten in multiple porcine and human models with hypertrophic cardiomyopathy. *British Journal of Pharmacology*, 1–18. https://doi.org/10.1111/bph.70247